Effects of Heat and Mass Transfer on Peristaltic Flow of Carreau Fluid in a Vertical Annulus

Sohail Nadeem and Noreen Sher Akbar

Department of Mathematics, Quaid-i-Azam University 45320, Islamabad 44000, Pakistan

Reprint requests to S. N.; E-mail: snqau@hotmail.com

Z. Naturforsch. **65a,** 781 – 792 (2010); received June 10, 2009 / revised November 6, 2009

This article is devoted to the study of peristaltic transport of a Carreau fluid in a vertical annulus under the consideration of long wavelength. The flow is investigated in a wave frame of reference moving with the velocity of the wave. Exact solutions have been evaluated for temperature and concentration field, while approximated analytical and numerical solutions are found for the velocity field using (i) the perturbation method and (ii) the shooting method. The effects of various emerging parameters are investigated graphically.

Key words: Peristaltic Flow; Carreau Fluid; Annulus; Perturbation Solution; Numerical Solutions.

1. Introduction

Peristalsis is an important mechanism for transporting fluids. The word peristalsis comes from the Greek word peristalikos, which means clasping and compressing. Peristaltic transport is a form of fluid transport induced by a progressive wave of area contraction or expansion along the length of a distensible tube containing fluids. In physiology, peristalsis used by the body to propel or mix the contents of a tube as in ureter, gastro-intestinal tract, bile duct, and other glandular ducts. Some worms use peristalsis as a means of locomotion. Peristalsis mechanism has attracted the attention of many researcher's since the first investigation of Latham [1]. A number of exact, analytical, and numerical studies of peristaltic transport for Newtonian and non-Newtonian fluids have been investigated in references [2 – 9].

In the literature, numerous studies regarding peristaltic motion have been done for Newtonian fluids. But such approach fails to give proper understanding of peristalsis in blood vessels, chyme movement in intestine, semen transport in ductus afferents of male reproductive tract, and transport of spermatozoa in cervical canal. In these body organs, the fluid viscosity varies across the thickness of the duct. Most of the physiological fluid do not behave like a Newtonian fluid in reality. Limited studies [10 – 16] are available in literature for peristalsis involving non-Newtonian fluids.

To the best of our knowledge only one article [17] exist in peristaltic literature which studies the peristaltic flow in connection with mixed convection heat and mass transfer. Mixed convection is the combination of free convection and forced convection. Free convection is occurred due to temperature difference in a fluid at different locations, while forced convection is the flow of heat due to some externally applied forces.

Keeping in mind the importance of peristaltic mechanism in connection with mixed convection heat and mass transfer, we present the effects of mixed convection heat and mass transfer on peristaltic flow of a Carreau fluid in a vertical annulus. Exact solutions have been calculated for energy and concentration while analytical and numerical solutions have been presented for the velocity profile. At the end of the article graphical results have been presented for various parameter of interest.

2. Mathematical Model

For an incompressible fluid the balance of mass and momentum are given by

$$\operatorname{div}\mathbf{V} = 0, \tag{1}$$

$$\rho\frac{\mathrm{d}\mathbf{V}}{\mathrm{d}t} = -P\mathbf{I} + \operatorname{div}\bar{\boldsymbol{\tau}}_{ij} + \rho\mathbf{f}, \tag{2}$$

where ρ is the density, $\mathbf{V}$ is the velocity vector, $-P\mathbf{I}$ is the spherical part of the stress due to constraint of incompressibility, $\bar{\boldsymbol{\tau}}_{ij}$ is the Cauchy stress tensor, $\mathbf{f}$ re-

0932–0784 / 10 / 1000–0781 $ 06.00

presents the specific body force and $\mathrm{d}/\mathrm{d}t$ represents the material time derivative. The constitutive equation for a Carreau fluid is given by [2]

$$\frac{(\eta-\eta_\infty)}{(\eta_0-\eta_\infty)} = \left[1+(\Gamma\bar{\dot\gamma})^2\right]^{\frac{(n-1)}{2}}, \tag{3}$$

$$\bar{\boldsymbol{\tau}}_{ij} = \eta_0\left[1+\frac{(n-1)}{2}(\Gamma\bar{\dot\gamma})^2\right]\bar{\dot\gamma}_{ij}, \tag{4}$$

in which $\bar{\boldsymbol{\tau}}_{ij}$ is the extra stress tensor, η_∞ is the infinite shear rate viscosity, η_0 is the zero shear rate viscosity, Γ is the time constant, n is the power law index, and $\dot\gamma$ is defined as

$$\bar{\dot\gamma} = \sqrt{\frac{1}{2}\sum_i\sum_j \bar{\dot\gamma}_{ij}\bar{\dot\gamma}_{ij}} = \sqrt{\frac{1}{2}\boldsymbol{\Pi}}. \tag{5}$$

Here $\boldsymbol{\Pi}$ is the second invariant strain tensor.

3. Mathematical Formulation

Let us consider the peristaltic flow of an incompressible Carreau fluid in a vertical annulus. The inner tube is rigid and maintained at temperature $\bar{T}_1$, the outer tube has a sinusoidal wave travelling down its walls and maintained at temperature $\bar{T}_0$. The geometry of the wall surface is defined as

$$\bar{R}_1 = a_1, \tag{6}$$

$$\bar{R}_2 = a_2 + b\sin\frac{2\pi}{\lambda}(\bar{Z}-c\bar{t}), \tag{7}$$

where a_1 is the radius of the inner tube, a_2 is the radius of the outer tube at inlet, b is the wave amplitude, λ is the wavelength, c the wave speed, and $\bar{t}$ the time (see Fig. 1).

The governing equations of Carreau fluid along with heat and mass transfer are

$$\frac{\partial\bar{U}}{\partial\bar{R}}+\frac{\bar{U}}{\bar{R}}+\frac{\partial\bar{W}}{\partial\bar{Z}} = 0, \tag{8}$$

$$\begin{aligned}&\rho\left(\frac{\partial}{\partial\bar{t}}+\bar{U}\frac{\partial}{\partial\bar{R}}+\bar{W}\frac{\partial}{\partial\bar{Z}}\right)\bar{U}\\ &= -\frac{\partial\bar{p}}{\partial\bar{R}}+\left(\frac{1}{\bar{R}}\frac{\partial}{\partial\bar{R}}(\bar{R}\bar{\boldsymbol{\tau}}_{11})+\frac{\partial}{\partial\bar{Z}}(\bar{\boldsymbol{\tau}}_{31})-\frac{\bar{\boldsymbol{\tau}}_{22}}{\bar{R}}\right),\end{aligned} \tag{9}$$

$$\begin{aligned}&\rho\left(\frac{\partial}{\partial\bar{t}}+\bar{U}\frac{\partial}{\partial\bar{R}}+\bar{W}\frac{\partial}{\partial\bar{Z}}\right)\bar{W}\\ &= -\frac{\partial\bar{p}}{\partial\bar{Z}}+\left(\frac{1}{\bar{R}}\frac{\partial}{\partial\bar{R}}(\bar{R}\bar{\boldsymbol{\tau}}_{13})+\frac{\partial}{\partial\bar{Z}}(\bar{\boldsymbol{\tau}}_{33})\right)\\ &\quad+\rho g\alpha(\bar{T}-\bar{T}_0)+\rho g\alpha(\bar{C}-\bar{C}_0),\end{aligned} \tag{10}$$

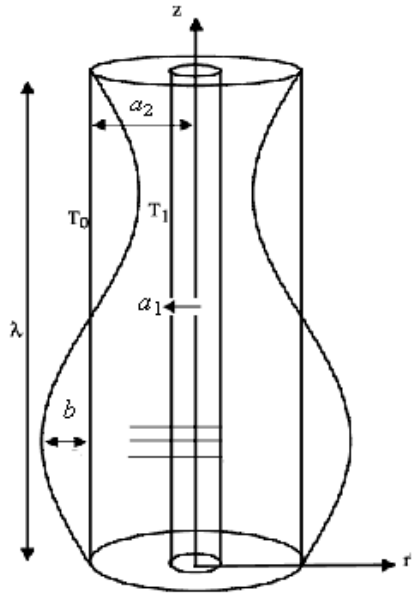

Fig. 1. Geometry of the problem.

$$\begin{aligned}&\rho c_{\mathrm{p}}\left(\frac{\partial}{\partial\bar{t}}+\bar{U}\frac{\partial}{\partial\bar{R}}+\bar{W}\frac{\partial}{\partial\bar{Z}}\right)\bar{T}\\ &= k\left(\frac{\partial^2\bar{T}}{\partial\bar{R}^2}+\frac{1}{\bar{R}}\frac{\partial\bar{T}}{\partial\bar{R}}+\frac{\partial^2\bar{T}}{\partial\bar{Z}^2}\right),\end{aligned} \tag{11}$$

$$\begin{aligned}&\left(\frac{\partial}{\partial\bar{t}}+\bar{U}\frac{\partial}{\partial\bar{R}}+\bar{W}\frac{\partial}{\partial\bar{Z}}\right)\bar{C}\\ &= D\left(\frac{\partial^2\bar{C}}{\partial\bar{R}^2}+\frac{1}{\bar{R}}\frac{\partial\bar{C}}{\partial\bar{R}}+\frac{\partial^2\bar{C}}{\partial\bar{Z}^2}\right)\\ &\quad+\frac{DK_{\mathrm{T}}}{T_{\mathrm{m}}}\left(\frac{\partial^2\bar{T}}{\partial\bar{R}^2}+\frac{1}{\bar{R}}\frac{\partial\bar{T}}{\partial\bar{R}}+\frac{\partial^2\bar{T}}{\partial\bar{Z}^2}\right).\end{aligned} \tag{12}$$

In the above equations, $\bar{P}$ is the pressure, $\bar{U}$, $\bar{W}$ are the velocity components in the radial and axial directions, respectively, $\bar{T}$ is the temperature, $\bar{C}$ is the concentration of the fluid, $\bar{T}_0$ is the constant temperature of the inner tube, $\bar{C}_0$ is the constant concentration of inner tube, ρ is the density, k denotes the thermal conductivity, c_{p} is the specific heat at constant pressure, T_{m} is the temperature of the medium, D is the coefficients of mass diffusivity, K_{T} is the thermal-diffusion ratio.

In the fixed coordinates $(\bar{R},\bar{Z})$, the flow between the two tubes is unsteady. It becomes steady in a wave frame $(\bar{r},\bar{z})$ moving with the same speed as the wave moves in the $\bar{Z}$-direction. The transformations between the two frames are

$$\begin{aligned}&\bar{r} = \bar{R}, \quad \bar{z} = \bar{Z}-c\bar{t},\\ &\bar{u} = \bar{U}, \quad \bar{w} = \bar{W}-c,\end{aligned} \tag{13}$$

where $\bar{u}$ and $\bar{w}$ are the velocities in the wave frame.

The appropriate boundary conditions in the wave frame are of the following form:

$$\bar{w} = -1 \text{ at } \bar{r} = \bar{r}_1, \tag{14a}$$

$$\bar{w} = -1 \text{ at } \bar{r} = \bar{r}_2, \tag{14b}$$

$$\bar{T} = \bar{T}_0 \text{ at } \bar{r} = \bar{r}_1, \tag{14c}$$

$$\bar{T} = \bar{T}_1 \text{ at } \bar{r} = \bar{r}_2, \tag{14d}$$

$$\bar{C} = \bar{C}_0 \text{ at } \bar{r} = \bar{r}_1, \tag{14e}$$

$$\bar{C} = \bar{C}_1 \text{ at } \bar{r} = \bar{r}_2, \tag{14f}$$

We introduce the dimensionless variables

$$\begin{aligned}
&R = \frac{\bar{R}}{a}, \quad r = \frac{\bar{r}}{a_2}, \quad Z = \frac{\bar{Z}}{\lambda}, \quad z = \frac{\bar{z}}{\lambda},\\
&W = \frac{\bar{W}}{c}, \quad w = \frac{\bar{w}}{c}, \quad \dot{\gamma} = \frac{a_2}{c}\bar{\dot{\gamma}}, \quad U = \frac{\lambda \bar{U}}{a_2 c},\\
&u = \frac{\lambda \bar{u}}{a_2 c}, \quad P = \frac{a_2^2 \bar{P}}{c\lambda\eta_0}, \quad \theta = \frac{(\bar{T}-\bar{T}_1)}{(\bar{T}_0-\bar{T}_1)},\\
&t = \frac{c\bar{t}}{\lambda}, \quad \delta = \frac{a_2}{\lambda}, \quad \mathrm{Re} = \frac{\rho c a_2}{\eta_0}, \quad \boldsymbol{\tau}_{11} = \frac{\lambda \bar{\boldsymbol{\tau}}_{11}}{c\eta_0},\\
&\boldsymbol{\tau}_{22} = \frac{\lambda \bar{\boldsymbol{\tau}}_{22}}{c\eta_0}, \quad \boldsymbol{\tau}_{33} = \frac{\lambda \bar{\boldsymbol{\tau}}_{33}}{c\eta_0}, \quad r_1 = \frac{\bar{r}_1}{a_2} = \varepsilon,\\
&r_2 = \frac{\bar{r}_2}{a_2} = 1 + \phi \sin(2\pi z), \quad \boldsymbol{\tau}_{13} = \boldsymbol{\tau}_{31} = \frac{a_2 \bar{\boldsymbol{\tau}}_{13}}{c\eta_0},\\
&\mathrm{We} = \frac{c\Gamma}{a_2}, \quad \beta = \frac{Q_0 a_2^2}{k(\bar{T}_1-\bar{T}_0)},\\
&\mathrm{Gr} = \frac{g\alpha a_2^3(\bar{T}_1-\bar{T}_0)}{\nu^2}, \quad \mathrm{Br} = \frac{\alpha g a^3(\bar{C}_1-\bar{C}_0)}{\nu^2},\\
&\mathrm{Sr} = \frac{\rho D K_{\mathrm{T}}(\bar{T}_0-\bar{T}_1)}{\eta_0 T_{\mathrm{m}}(\bar{C}_0-\bar{C}_1)}, \quad \mathrm{Sc} = \frac{\eta_0}{D\rho}, \quad \sigma = \frac{(\bar{C}-\bar{C}_1)}{(\bar{C}_0-\bar{C}_1)},
\end{aligned} \tag{15}$$

in which R and Z are the dimensionless form of radial and transverse components, respectively, Sr is the Soret number, Sc Schmidt number, Br is the local concentration Grashof number, Gr is the local temperature Grashof number, and We is the Weissenberg number.

Making use of (13) and (15), (9) to (12) take the form

$$\frac{\partial u}{\partial r} + \frac{u}{r} + \frac{\partial w}{\partial z} = 0, \tag{16}$$

$$\begin{aligned}
&\mathrm{Re}\,\delta^3 \left(u\frac{\partial}{\partial r} + w\frac{\partial}{\partial z}\right) u =\\
&-\frac{\partial P}{\partial r} + \delta^2 \left(\frac{1}{r}\frac{\partial}{\partial r}(r\boldsymbol{\tau}_{11}) + \frac{\partial}{\partial z}(\boldsymbol{\tau}_{31}) - \frac{\boldsymbol{\tau}_{22}}{r}\right),
\end{aligned} \tag{17}$$

$$\begin{aligned}
&\mathrm{Re}\,\delta \left(u\frac{\partial}{\partial r} + w\frac{\partial}{\partial z}\right) w =\\
&-\frac{\partial P}{\partial z} + \frac{1}{r}\frac{\partial}{\partial r}(r\boldsymbol{\tau}_{13}) + \delta^2 \frac{\partial}{\partial z}(\boldsymbol{\tau}_{33}) + \mathrm{Gr}\theta + \mathrm{Br}\sigma,
\end{aligned} \tag{18}$$

$$\begin{aligned}
&\mathrm{Re}\,\delta P_r \left(u\frac{\partial}{\partial r} + w\frac{\partial}{\partial z}\right) \theta =\\
&\frac{\partial^2 \theta}{\partial r^2} + \frac{1}{r}\frac{\partial \theta}{\partial r} + \delta^2 \frac{\partial^2 \theta}{\partial z^2} + \beta,
\end{aligned} \tag{19}$$

$$\begin{aligned}
&\mathrm{Re}\,\delta \left(u\frac{\partial}{\partial r} + w\frac{\partial}{\partial z}\right) \sigma\\
&= \frac{1}{\mathrm{Sc}} \left(\frac{1}{r}\frac{\partial}{\partial r}\left(r\frac{\partial \sigma}{\partial r}\right) + \delta^2 \frac{\partial^2 \sigma}{\partial z^2}\right)\\
&\quad + \mathrm{Sr} \left(\frac{1}{r}\frac{\partial}{\partial r}\left(r\frac{\partial \theta}{\partial r}\right) + \delta^2 \frac{\partial^2 \theta}{\partial z^2}\right),
\end{aligned} \tag{20}$$

where

$$\begin{aligned}
&\boldsymbol{\tau}_{ij} = \left[1 + \frac{(n-1)}{2}\mathrm{Re}^2 \dot{\gamma}^2\right] \dot{\gamma}_{ij}, \quad \dot{\gamma}_{11} = 2\frac{\partial u}{\partial r},\\
&\dot{\gamma}_{22} = \frac{2u}{r}, \quad \dot{\gamma}_{33} = 2\frac{\partial w}{\partial z},\\
&\dot{\gamma}_{13} = \dot{\gamma}_{31} = \left(\frac{\partial u}{\partial z}\delta^2 + \frac{\partial w}{\partial r}\right),\\
&\dot{\gamma} = \delta \sqrt{\frac{1}{2}\sum_i \sum_j \dot{\gamma}_{ij}\dot{\gamma}_{ij}}, \quad i = j,\\
&\dot{\gamma} = \sqrt{\frac{1}{2}\sum_i \sum_j \dot{\gamma}_{ij}\dot{\gamma}_{ij}}, \quad i \neq j,\\
&\boldsymbol{\tau}_{13} = \boldsymbol{\tau}_{31} = \left[1 + \frac{(n-1)}{2}\mathrm{Re}^2 \left(\frac{\partial w}{\partial r}\right)^2\right] \left(\frac{\partial w}{\partial r}\right).
\end{aligned} \tag{21}$$

Here δ, Re represent the wave and the Reynolds numbers, respectively. Under the assumptions of long wavelength $\delta \ll 1$ and low Reynolds number, i. e. neglecting the terms of order δ and higher, (17) to (20) take the form

$$\frac{\partial P}{\partial r} = 0, \tag{22}$$

$$\frac{\partial P}{\partial z} = -\frac{1}{r}\frac{\partial}{\partial r}(r\boldsymbol{\tau}_{31}) + \mathrm{Gr}\theta + \mathrm{Br}\sigma, \tag{23}$$

$$0 = \frac{\partial^2 \theta}{\partial r^2} + \frac{1}{r}\frac{\partial \theta}{\partial r} + \beta, \tag{24}$$

$$0 = \frac{1}{\mathrm{Sc}} \left(\frac{1}{r}\frac{\partial}{\partial r}\left(r\frac{\partial \sigma}{\partial r}\right)\right) + \mathrm{Sr} \left(\frac{1}{r}\frac{\partial}{\partial r}\left(r\frac{\partial \theta}{\partial r}\right)\right). \tag{25}$$

The corresponding boundary conditions are

$$w = -1, \text{ at } r = r_1 = \varepsilon, \tag{26a}$$

$$w = -1, \text{ at } r = r_2 = 1 + \phi \sin(2\pi z), \tag{26b}$$

$$\theta = 1, \text{ at } r = r_1, \tag{26c}$$

$$\theta = 0, \text{ at } r = r_2, \tag{26d}$$

$$\sigma = 1, \text{ at } r = r_1, \tag{26e}$$

$$\sigma = 0, \text{ at } r = r_2, \tag{26f}$$

4. Solution of the Problem

Solving (24) and (25) subject to the boundary conditions (26c) to (26f), we obtain the expression for temperature and concentration field as follows:

$$\theta(r,z) = \frac{1}{a_{11}}(a_{12}\ln(r) + a_{13}r^2 + a_{14}). \tag{27}$$

$$\begin{aligned}\sigma(r,z) = &-\frac{\mathrm{SrSc}}{a_{11}}(a_{12}\ln(r) + a_{13}r^2 + a_{14}) \\ &+ a_{17}\ln r + a_{18}.\end{aligned} \tag{28}$$

4.1. Perturbation Solution

To get the solution of (23), we employ the regular perturbation. For the perturbation solution, we expand w, Q, and P as

$$w = w_0 + \mathrm{We}^2 w_1 + O(\mathrm{We}^4), \tag{29a}$$

$$Q = Q_0 + \mathrm{We}^2 Q_1 + O(\mathrm{We}^4), \tag{29b}$$

$$P = P_0 + \mathrm{We}^2 P_1 + O(\mathrm{We}^4). \tag{29c}$$

The perturbation results for small parameter We^2 satisfying the conditions (26a) and (26b) for velocity fields and pressure gradient can be written as

$$\begin{aligned} w = &-1 + \left(\frac{r^2}{4} + a_{25}\ln r + a_{27}\right)\frac{\mathrm{d}P}{\mathrm{d}z} + a_{29}r^4 \\ &+ a_{30}r^2\ln r + a_{31}r^2 + a_{26}\ln r + a_{28} \\ &+ \mathrm{We}^2\Big[a_{58}r^{10} + a_{59}r^8 + a_{60}r^6 + a_{61}r^4 + a_{62}r^2 \\ &+ \frac{a_{63}}{r^2} + a_{65}r^2\ln r + a_{66}r^4\ln r + a_{67}r^6\ln r \\ &+ a_{68}r^8\ln r + a_{69}(\ln r)^2 + a_{70}r^2(\ln r)^2 \\ &+ a_{71}r^4(\ln r)^2 + a_{72}r^4(\ln r)^3 + a_{73}r^6(\ln r)^2 \\ &+ a_{76}\ln r + a_{77}\Big]. \end{aligned} \tag{30}$$

$$\frac{\mathrm{d}P}{\mathrm{d}z} = \frac{2Q + r_2^2 - r_1^2 - a_{78}}{a_{77}} + \mathrm{We}^2\left(-\frac{a_{79}}{a_{77}}\right). \tag{31}$$

The pressure rise ΔP and the friction force F on inner and outer tubes, $F^{(0)}$, $F^{(i)}$, are given by

$$\Delta P = \int_0^1 \frac{\mathrm{d}P}{\mathrm{d}z}\mathrm{d}z, \tag{32}$$

$$F^{(0)} = \int_0^1 r_1^2\left(-\frac{\mathrm{d}P}{\mathrm{d}z}\right)\mathrm{d}z, \tag{33}$$

$$F^{(i)} = \int_0^1 r_2^2\left(-\frac{\mathrm{d}P}{\mathrm{d}z}\right)\mathrm{d}z, \tag{34}$$

where $\frac{\mathrm{d}P}{\mathrm{d}z}$ is defined in (31).

The dimensionless expressions for the five considered wave forms are given by the following equations:

1. Sinusoidal wave:

$$r_2(z) = 1 + \phi\sin(2\pi z).$$

2. Triangular wave:

$$r_2(z) = 1 + \phi\left\{\frac{8}{\pi^3}\sum_{n=1}^{\infty}\frac{(-1)^{n+1}}{(2n-1)}\sin(2\pi(2n-1)z)\right\}.$$

3. Square wave:

$$r_2(z) = 1 + \phi\left\{\frac{4}{\pi}\sum_{n=1}^{\infty}\frac{(-1)^{n+1}}{(2n-1)}\cos(2\pi(2n-1)z)\right\}.$$

4. Trapezoidal wave:

$$r_2(z) = 1 + \phi\left\{\frac{32}{\pi^2}\sum_{n=1}^{\infty}\frac{\sin\frac{\pi}{8}(2n-1)}{(2n-1)^2}\sin(2\pi(2n-1)z)\right\}.$$

5. Multi sinusoidal wave:

$$h(z) = 1 + \phi\sin(2m\pi z).$$

4.2. Numerical Solution

The present problem consisting of (23) and (26) is also solved numerically by employing the shooting method. The numerical results are compared with the perturbation results (see Fig. 2 and Table 1).

5. Numerical Results and Discussion

In this section we present the solution for the Carreau fluid graphically. The expression for pressure rise ΔP is calculated numerically using mathematics

Table. 1. Shows numerical values of comparison of axial velocity for perturbation and numerical solutions when $\varepsilon = 0.1$, We $= 0.1$, $z = 0.1$, $dP/dz = 0.3$, $\phi = 0.3$, Sr $= 0.5$, Sc $= 0.3$, $\beta = 0.08$, Gr $= 0.02$, Br $= 0.01$, $n = 0.1$.

r	Numerical solution	Perturbation solution	Error
0.1	−1.00000	−1.00000	0.00000
0.2	−1.07808	−1.07369	0.00408
0.3	−1.12036	−1.11360	0.00607
0.4	−1.13952	−1.13170	0.00690
0.5	−1.14701	−1.13878	0.00722
0.6	−1.14552	−1.13737	0.00716
0.7	−1.13504	−1.12749	0.00669
0.8	−1.11861	−1.11197	0.00597
0.9	−1.09611	−1.09073	0.00493
1.0	−1.06444	−1.06084	0.00339
1.1	−1.03022	−1.02853	0.00164
1.18	−1.00000	−1.00000	0.00000

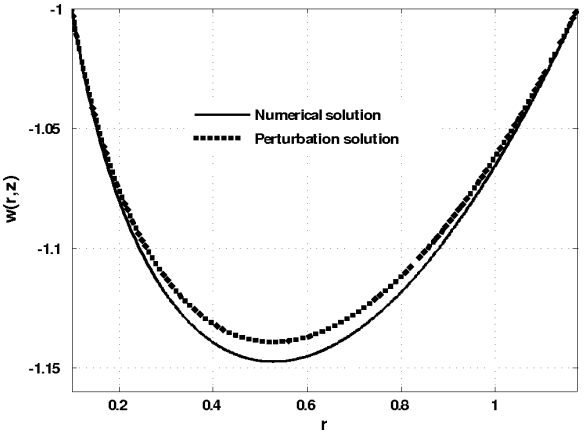

Fig. 2. Comparison of velocity field for $\varepsilon = 0.1$, We $= 0.1$, $z = 0.1$, $dP/dz = 0.3$, $\phi = 0.3$, Sr $= 0.5$, Sc $= 0.3$, $\beta = 0.08$, Gr $= 0.02$, Br $= 0.01$, $n = 0.1$.

software. The effects of various parameters on the pressure rise ΔP are shown in Figures 3 to 6 for various values of Weissenberg number We, amplitude ratio ϕ, radius ratio ε, and power law index n. It is observed from these figures that the pressure rise increases with the increase in We, ϕ, ε, while the pressure rise decreases with increase in n. The peristaltic pumping region is $(-2 \leq Q \leq -1.5)$ for Figure 3, $(-2 \leq Q \leq 0.2)$ for Figure 4, $(-2 \leq Q \leq -0.3)$ for Figure 5, and $(-2 \leq Q \leq 1)$ for Figure 6, otherwise, there is augmented pumping. Figures 7 to 14 represent the behaviour of the frictional forces. It is depicted that these forces have an opposite behaviour as compared with the pressure rise. Figure 15 is prepared to see the behaviour of different wave forms on pressure rise. It is analyzed that a square wave has the best pumping characteristics while a triangular wave has the worst pumping characteristics. Effects of temperature profile are shown through

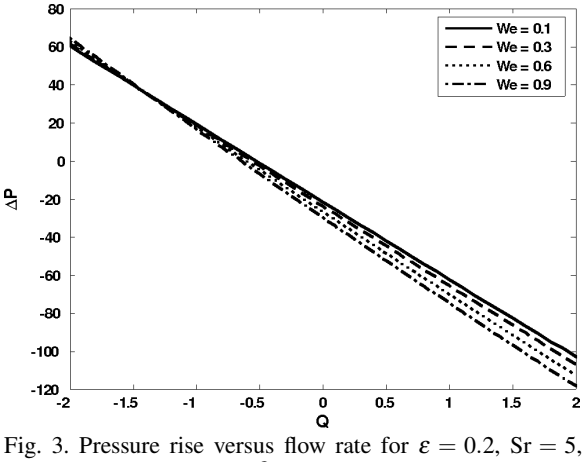

Fig. 3. Pressure rise versus flow rate for $\varepsilon = 0.2$, Sr $= 5$, Sc $= 0.2$, Gr $= 2$, Br $= 3$, $\beta = 0.04$, $\phi = 0.1$, $n = 0.1$.

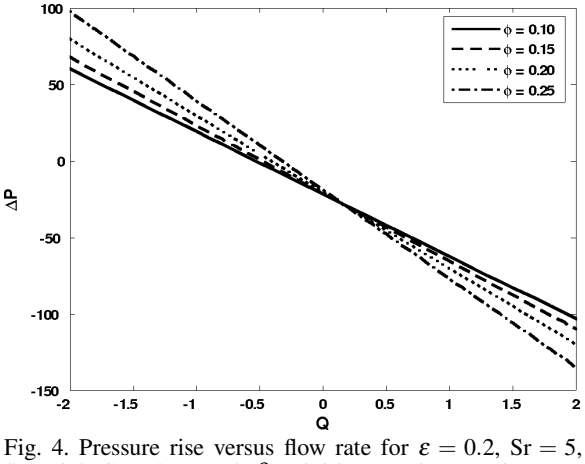

Fig. 4. Pressure rise versus flow rate for $\varepsilon = 0.2$, Sr $= 5$, Sc $= 0.2$, Gr $= 2$, Br $= 3$, $\beta = 0.04$, We $= 0.1$, $n = 0.1$.

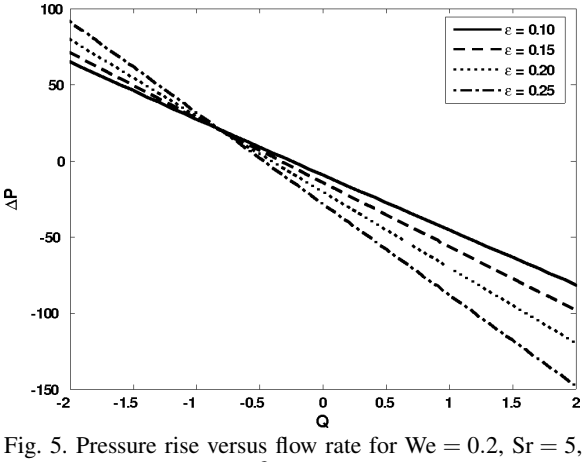

Fig. 5. Pressure rise versus flow rate for We $= 0.2$, Sr $= 5$, Sc $= 0.2$, Gr $= 2$, Br $= 3$, $\beta = 0.04$, $n = 0.1$.

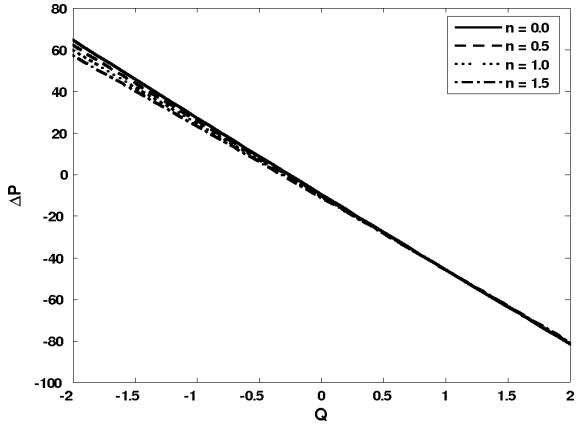

Fig. 6. Pressure gradient versus flow rate for We = 0.2, Sr = 5, Sc = 0.2, Gr = 2, Br = 3, $\beta = 2$, $\varepsilon = 0.1$.

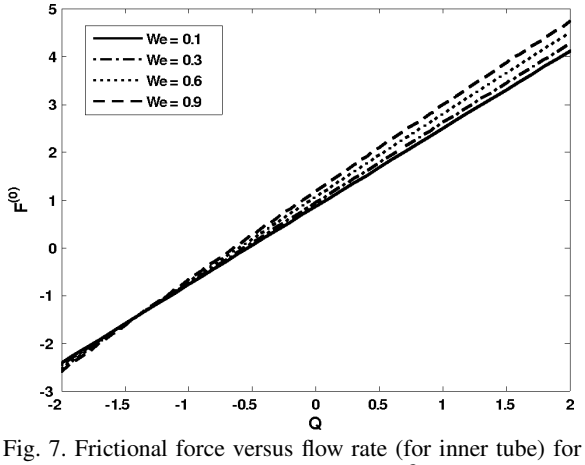

Fig. 7. Frictional force versus flow rate (for inner tube) for $\varepsilon = 0.2$, Sr = 5, Sc = 0.2, Gr = 2, Br = 3, $\beta = 0.04$, $\phi = 0.1$, $n = 0.1$.

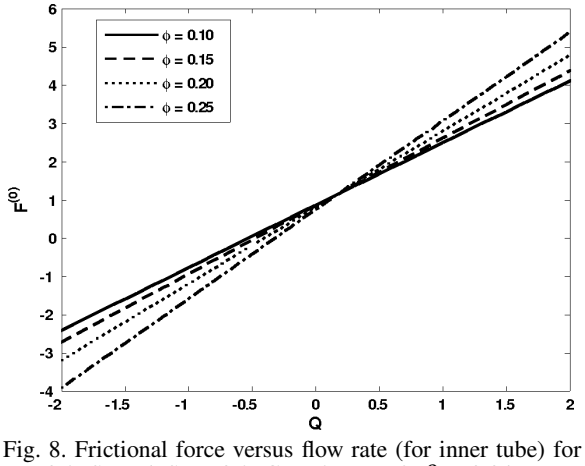

Fig. 8. Frictional force versus flow rate (for inner tube) for $\varepsilon = 0.2$, Sr = 5, Sc = 0.2, Gr = 2, Br = 3, $\beta = 0.04$, We = 0.1, $n = 0.1$.

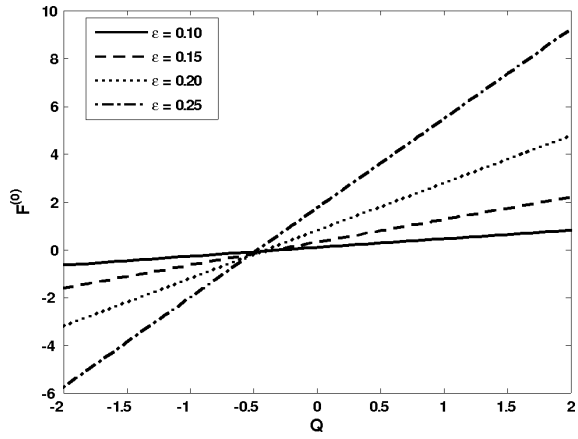

Fig. 9. Frictional force versus flow rate (for inner tube) for We = 0.2, Sr = 5, Sc = 0.2, Gr = 2, Br = 3, $\beta = 0.04$, $n = 0.1$.

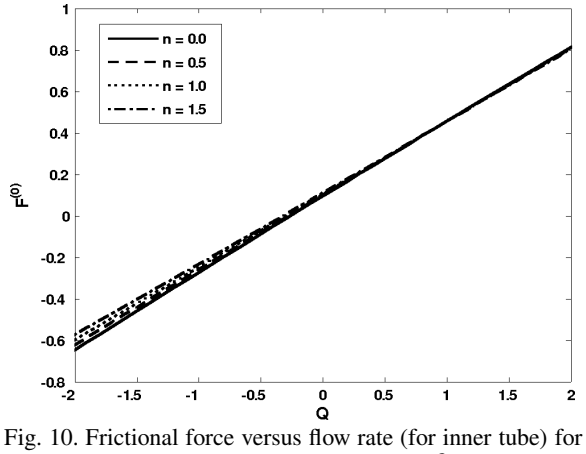

Fig. 10. Frictional force versus flow rate (for inner tube) for We = 0.2, Sr = 5, Sc = 0.2, Gr = 2, Br = 3, $\beta = 2$, $\varepsilon = 0.1$.

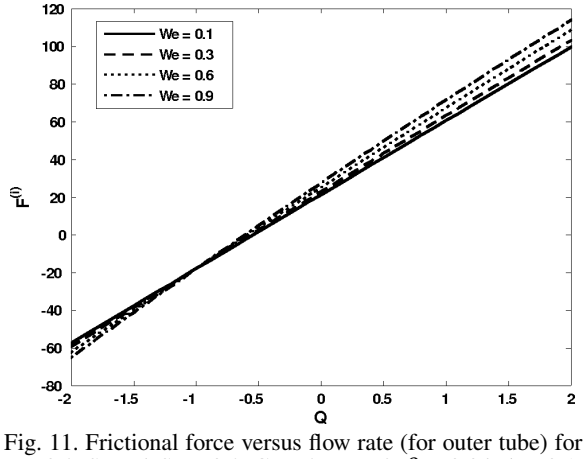

Fig. 11. Frictional force versus flow rate (for outer tube) for $\varepsilon = 0.2$, Sr = 5, Sc = 0.2, Gr = 2, Br = 3, $\beta = 0.04$, $\phi = 0.1$, $n = 0.1$.

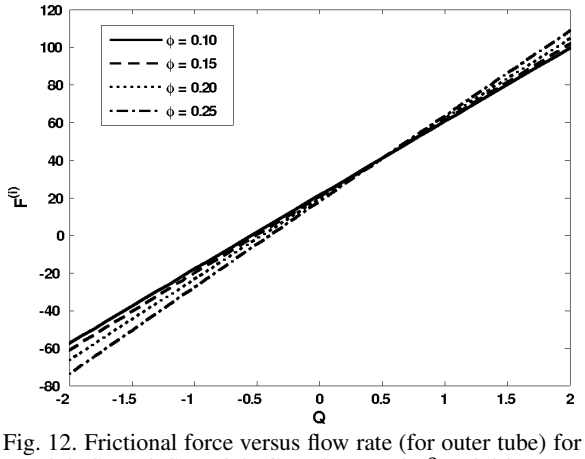

Fig. 12. Frictional force versus flow rate (for outer tube) for $\varepsilon = 0.2$, Sr $= 5$, Sc $= 0.2$, Gr $= 2$, Br $= 3$, $\beta = 0.04$, We $= 0.1$, $n = 0.1$.

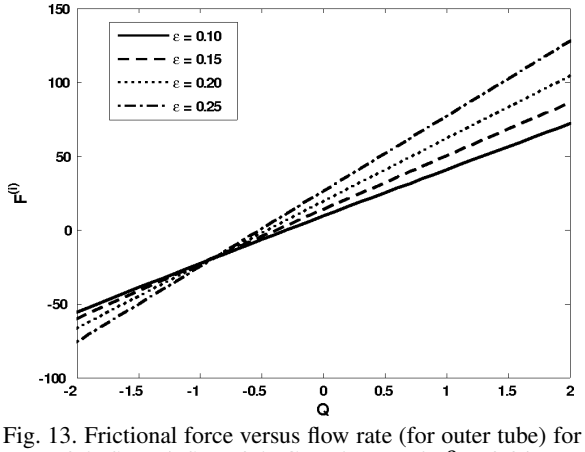

Fig. 13. Frictional force versus flow rate (for outer tube) for We $= 0.2$, Sr $= 5$, Sc $= 0.2$, Gr $= 2$, Br $= 3$, $\beta = 0.04$, $n = 0.1$.

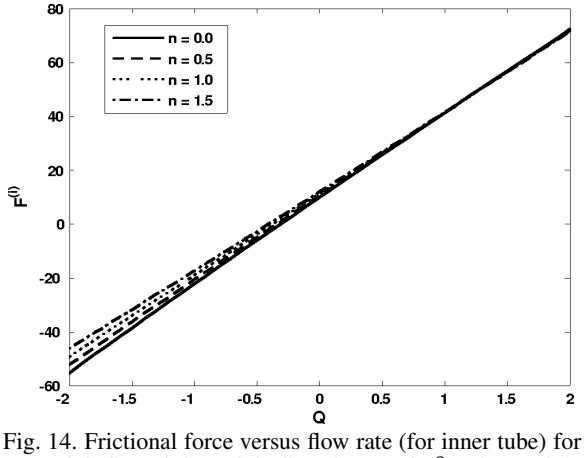

Fig. 14. Frictional force versus flow rate (for inner tube) for We $= 0.2$, Sr $= 5$, Sc $= 0.2$, Gr $= 2$, Br $= 3$, $\beta = 2$, $\varepsilon = 0.1$.

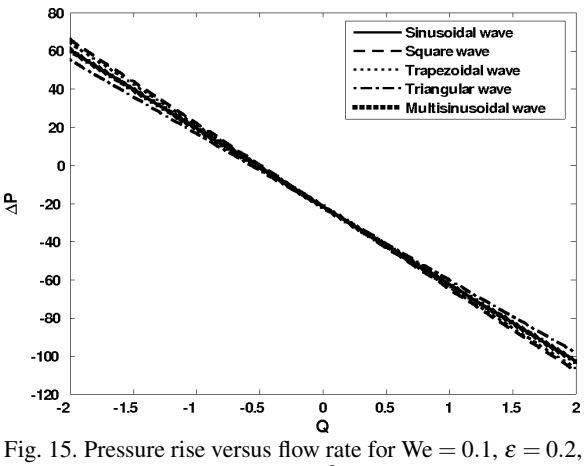

Fig. 15. Pressure rise versus flow rate for We $= 0.1$, $\varepsilon = 0.2$, Sr $= 5$, Sc $= 0.2$, Gr $= 2$, Br $= 3$, $\beta = 0.04$, $\phi = 0.1$, $n = 0.1$.

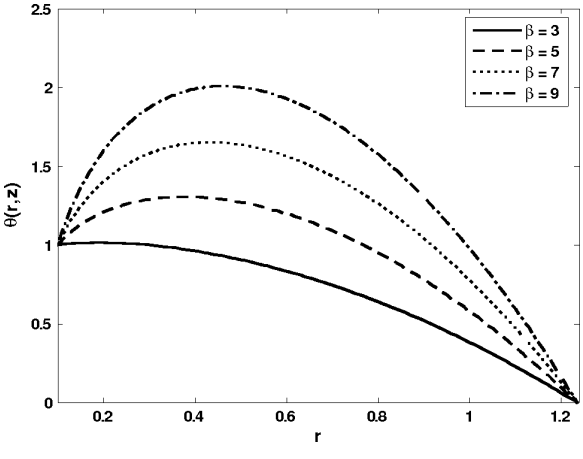

Fig. 16. Temperature profile for $\phi = 0.4$, $\varepsilon = 0.1$, $z = 0.1$.

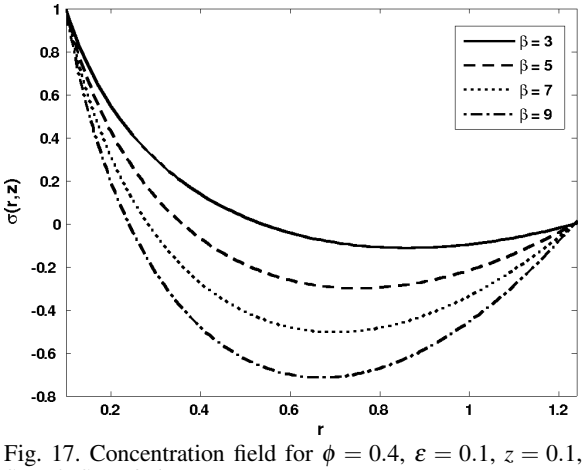

Fig. 17. Concentration field for $\phi = 0.4$, $\varepsilon = 0.1$, $z = 0.1$, Sr $= 3$, Sc $= 0.5$.

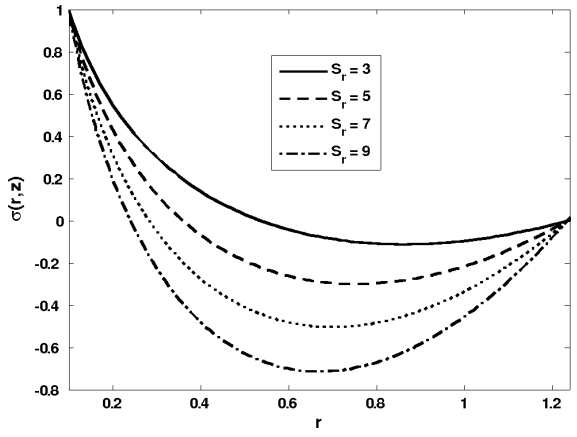

Fig. 18. Concentration field for $\phi = 0.4$, $\varepsilon = 0.1$, $z = 0.1$, $\beta = 3$, Sc $= 0.5$.

Figure 16. It is seen that with the increase in β the temperature profile increases. The concentration field σ for different values of β, Sr, and Sc are shown in Figures 17 to 19. We observed that the concentration field decreases with the increase in β (heat source parameter), Sr (Soret number), and Sc (Schmidth number). Figures 20 to 24 are prepared to see the behaviour of pressure gradient for different wave shapes. It is observed from the figures that for $z \in [0, 0.5]$ and $[1.1, 1.5]$ the pressure gradient is small, and large pressure gradient occurs for $z \in [0.51, 1]$, moreover, it is seen that with the increase in ϕ the pressure gradient increases. Figure 25 shows the streamlines for different wave forms. It is observed that the size of the trapped bolus in a triangular wave is small as compared with the other wave forms.

Acknowledgement

The authors are thankful to Higher Education Commission for the financial support of this work.

6. Appendix

$$a_{11} = 4(\ln(r_1) - \ln(r_2)),$$

$$a_{12} = 4 + \beta(r_1^2 - r_2^2),$$

$$a_{13} = \beta(\ln(r_2) - \ln(r_1)),$$

$$a_{14} = \beta(r_2^2 \ln(r_1) - r_1^2 \ln(r_2)) - 4\ln(r_2),$$

$$a_{15} = -\frac{\mathrm{SrSc}}{a_{11}}(a_{12}\ln(r_1) + a_{13}r_1^2 + a_{14}),$$

$$a_{16} = -\frac{\mathrm{SrSc}}{a_{11}}(a_{12}\ln(r_2) + a_{13}r_2^2 + a_{14}),$$

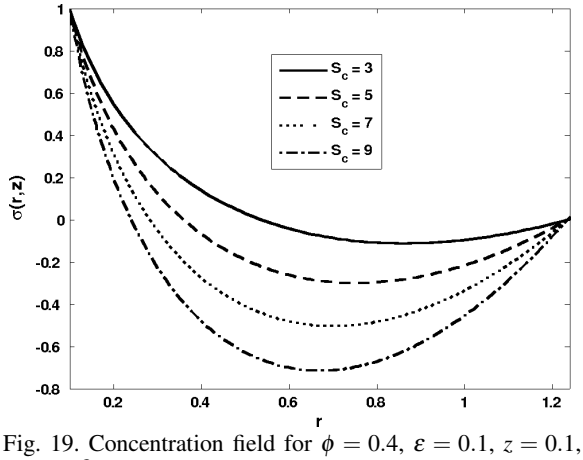

Fig. 19. Concentration field for $\phi = 0.4$, $\varepsilon = 0.1$, $z = 0.1$, Sr $= 3$, $\beta = 0.5$.

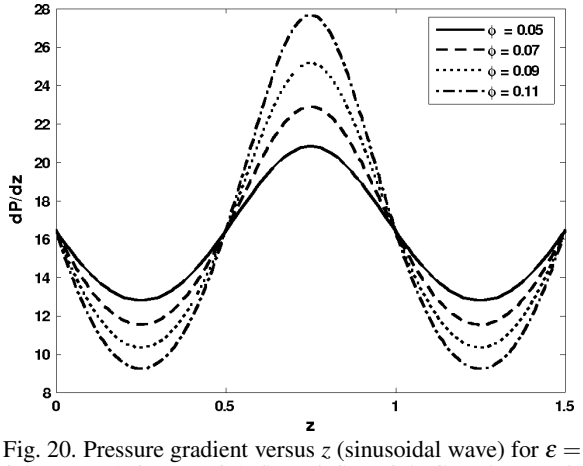

Fig. 20. Pressure gradient versus z (sinusoidal wave) for $\varepsilon = 0.2$, $Q = -1.5$, We $= 0.1$, Sr $= 5$, Sc $= 0.2$, Gr $= 2$, Br $= 3$, $\beta = 0.04$.

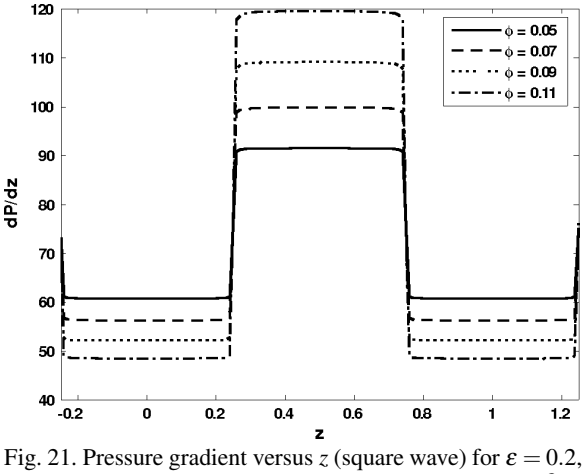

Fig. 21. Pressure gradient versus z (square wave) for $\varepsilon = 0.2$, $Q = -1.5$, We $= 0.1$, Sr $= 5$, Sc $= 0.2$, Gr $= 2$, Br $= 3$, $\beta = 0.04$.

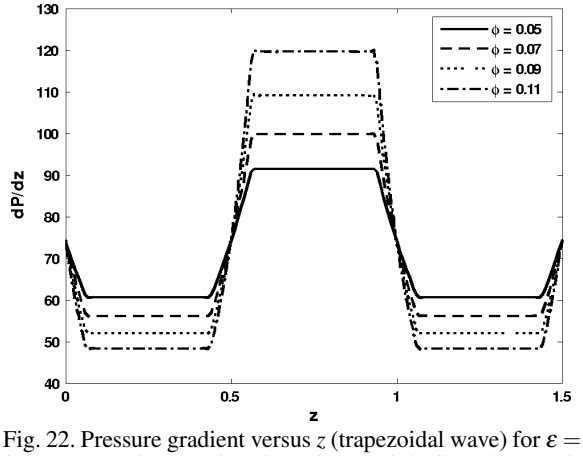

Fig. 22. Pressure gradient versus z (trapezoidal wave) for $\varepsilon = 0.2$, $Q = -1.5$, We $= 0.1$, Sr $= 5$, Sc $= 0.2$, Gr $= 2$, Br $= 3$, $\beta = 0.04$.

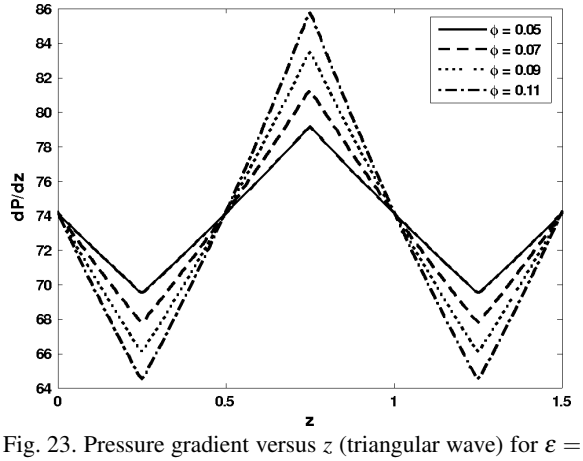

Fig. 23. Pressure gradient versus z (triangular wave) for $\varepsilon = 0.2$, $Q = -1.5$, We $= 0.1$, Sr $= 5$, Sc $= 0.2$, Gr $= 2$, Br $= 3$, $\beta = 0.04$.

$$a_{17} = \frac{1 - a_{15} - a_{16}}{(\ln(r_1) - \ln(r_2))},$$

$$a_{18} = 1 - a_{15} - a_{17}\ln r_1,$$

$$a_{19} = \frac{\mathrm{Gr}a_{13}}{a_{11}} - \frac{\mathrm{SrScBr}a_{13}}{a_{11}},$$

$$a_{20} = \frac{\mathrm{Gr}a_{12}}{a_{11}} - \left(\frac{2Sr\mathrm{ScBr}a_{12}}{a_{11}}\right) + \mathrm{Br}a_{17},$$

$$a_{21} = \frac{\mathrm{Gr}a_{14}}{a_{11}} - \frac{\mathrm{SrScBr}a_{14}}{a_{11}} + \mathrm{Br}a_{18},$$

$$a_{22} = a_{29}r_1^4 + a_{30}r_1^2\ln r_1 + a_{31}r_1^2,$$

$$a_{23} = a_{29}r_2^4 + a_{30}r_2^2\ln r_2 + a_{31}r_2^2,$$

$$a_{24} = a_{29}r_2^4 + a_{30}r_1^2\ln r_1$$

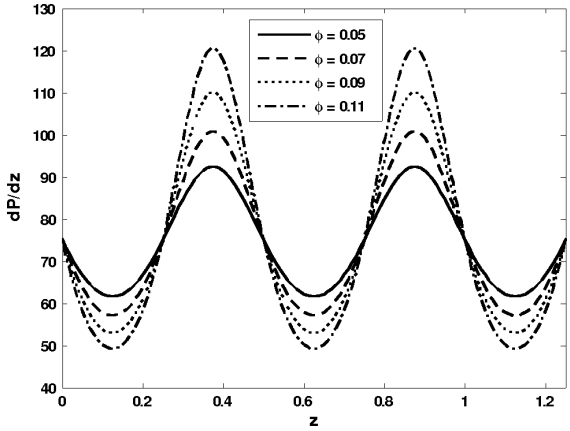

Fig. 24. Pressure gradient versus z (multisinusoidal wave) for $\varepsilon = 0.2$, $Q = -1.5$, We $= 0.1$, Sr $= 5$, Sc $= 0.2$, Gr $= 2$, Br $= 3$, $\beta = 0.04$.

$$a_{25} = \frac{r_1^2 - r_2^2}{4(\ln(r_1) - \ln(r_2))},$$

$$a_{26} = a_{22} - a_{23},$$

$$a_{27} = -\frac{(r_2^2 + r_1^2)}{8} - a25(\ln r_1 + \ln r_2),$$

$$a_{28} = -\frac{(1 + a_{22} + a_{23} + a_{26}(\ln r_1 + \ln r_2))}{2},$$

$$a_{29} = -\frac{a_{19}}{16},$$

$$a_{30} = -\frac{a_{20}}{4},$$

$$a_{31} = \frac{a_{20}}{4} - \frac{a_{21}}{4},$$

$$a_{32} = a_{30} + 2a_{31},$$

$$a_{33} = 16(a_{29})^2,$$

$$a_{34} = \frac{\mathrm{d}P_0}{\mathrm{d}z}(4a_{29} + 8a_{32}a_{29}),$$

$$a_{35} = \frac{\mathrm{d}P_0}{\mathrm{d}z}a_{32} + \frac{1}{4}\left(\frac{\mathrm{d}P_0}{\mathrm{d}z}\right)^2 + 8\left(\frac{\mathrm{d}P_0}{\mathrm{d}z}\right)a_{25}a_{29} + 8a_{29}a_{26} + a_{32}a_{32},$$

$$a_{36} = \left(\frac{\mathrm{d}P_0}{\mathrm{d}z}\right)^2 a_{25} + \left(\frac{\mathrm{d}P_0}{\mathrm{d}z}\right)a_{26} + 2\left(\frac{\mathrm{d}P_0}{\mathrm{d}z}\right)a_{25}a_{32} + 2a_{26}a_{32},$$

$$a_{37} = 4\left(\frac{\mathrm{d}P_0}{\mathrm{d}z}\right)a_{30}a_{25} + 4a_{30}a_{26},$$

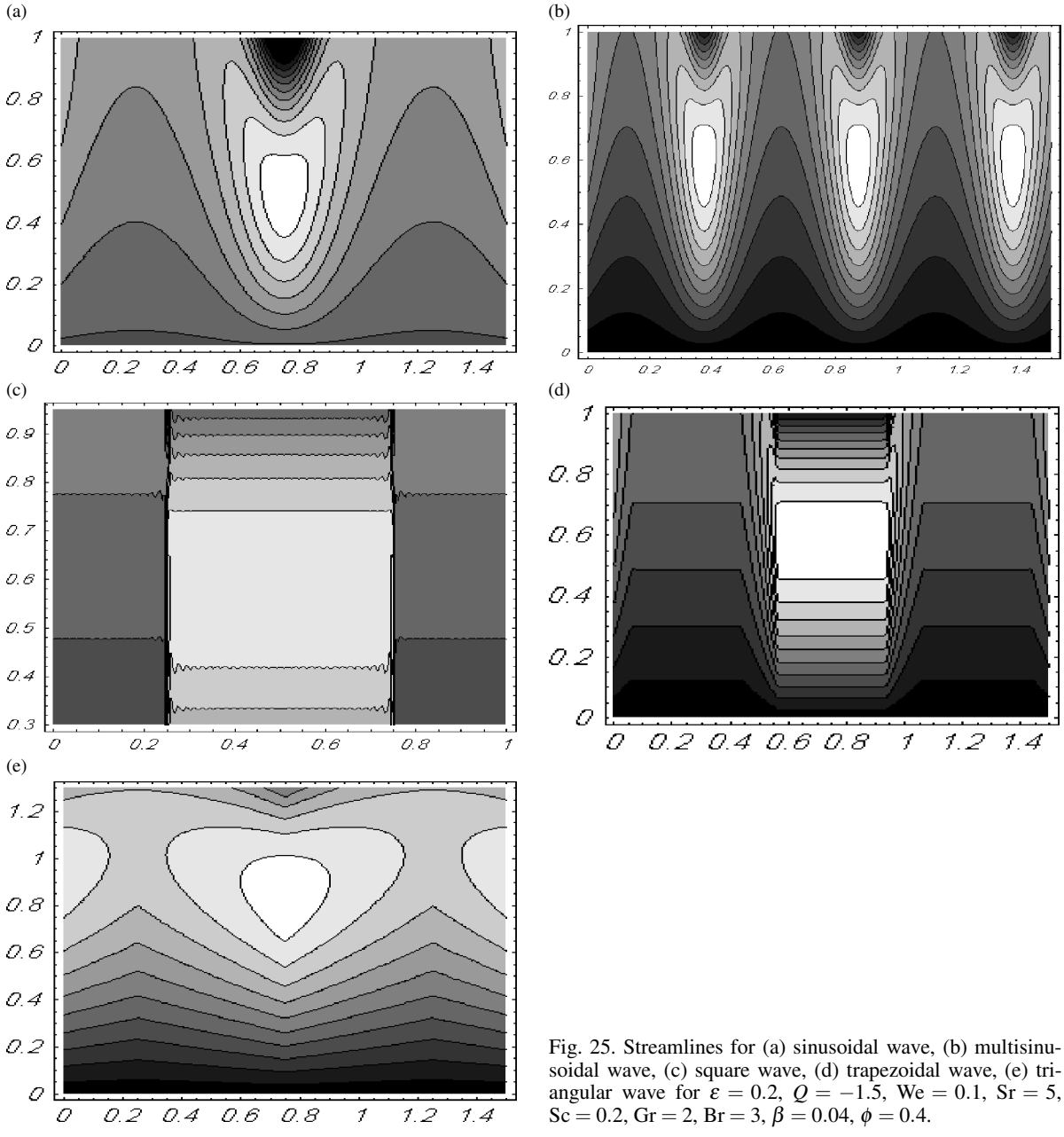

Fig. 25. Streamlines for (a) sinusoidal wave, (b) multisinusoidal wave, (c) square wave, (d) trapezoidal wave, (e) triangular wave for $\varepsilon = 0.2$, $Q = -1.5$, We $= 0.1$, Sr $= 5$, Sc $= 0.2$, Gr $= 2$, Br $= 3$, $\beta = 0.04$, $\phi = 0.4$.

$$a_{38} = 2\left(\frac{\mathrm{d}P_0}{\mathrm{d}z}\right) a_{30} + 4a_{30}a_{32},$$

$$a_{39} = a_{29}a_{30},$$

$$a_{40} = 4(a_{30})^2,$$

$$a_{41} = \left(\frac{\mathrm{d}P_0}{\mathrm{d}z}\right)^2 (a_{25})^2 + 2\left(\frac{\mathrm{d}P_0}{\mathrm{d}z}\right) a_{26}a_{25} + (a_{26})^2,$$

$$a_{42} = 4a_{29}a_{33},$$

$$a_{43} = \frac{\mathrm{d}P_0}{\mathrm{d}z}\frac{1}{2}a_{33} + (a_{30} + 2a_{31})a_{33} + 4a_{29}a_{34},$$

$$a_{44} = \frac{\mathrm{d}P_0}{\mathrm{d}z}\frac{1}{2}a_{34} + \frac{\mathrm{d}P_0}{\mathrm{d}z}a_{25}a_{33} + (a_{30} + 2a_{31})a_{34} + 4a_{29}a_{35} + a_{26}a_{33},$$

$$a_{45} = \frac{dP_0}{dz}\frac{1}{2}a_{35} + \frac{dP_0}{dz}a_{25}a_{34} + (a_{30}+2a_{31})a_{35} + 4a_{29}a_{36} + a_{26}a_{34},$$

$$a_{46} = \frac{dP_0}{dz}\frac{1}{2}a_{36} + \frac{dP_0}{dz}a_{25}a_{35} + (a_{30}+2a_{31})a_{36} + 4a_{29}a_{41} + a_{26}a_{35},$$

$$a_{47} = \frac{dP_0}{dz}\frac{1}{2}a_{41} + \frac{dP_0}{dz}a_{25}a_{36} + (a_{30}+2a_{31})a_{41} + a_{26}a_{36},$$

$$a_{48} = \frac{dP_0}{dz}a_{25}a_{41} + a_{26}a_{41},$$

$$a_{49} = \frac{dP_0}{dz}\frac{1}{2}a_{37} + \frac{dP_0}{dz}a_{25}a_{38} + (a_{30}+2a_{31})a_{37} + a_{26}a_{38} + 2a_{30}a_{36},$$

$$a_{50} = \frac{dP_0}{dz}\frac{1}{2}a_{38} + \frac{dP_0}{dz}a_{25}a_{39} + (a_{30}+2a_{31})a_{38} + a_{26}a_{39} + 2a_{30}a_{35} + 4a_{29}a_{37},$$

$$a_{51} = \frac{dP_0}{dz}\frac{1}{2}a_{39} + (a_{30}+2a_{31})a_{39} + 2a_{30}a_{34} + 4a_{29}a_{38},$$

$$a_{52} = 2a_{30}a_{33} + 4a_{29}a_{39},$$

$$a_{53} = \frac{dP_0}{dz}a_{25}a_{37} + 2a_{30}a_{41} + a_{26}a_{37},$$

$$a_{54} = \frac{dP_0}{dz}a_{25}a_{40} + 2a_{30}a_{37} + a_{26}a_{40},$$

$$a_{55} = \frac{1}{2}a_{39} + (a_{30}+2a_{31})a_{40} + 2a_{30}a_{38},$$

$$a_{56} = 2a_{30}a_{39} + 4a_{29}a_{40},$$

$$a_{57} = 2a_{30}a_{40},$$

$$a_{58} = -\frac{(n-1)}{20}a_{42},$$

$$a_{59} = -\frac{(n-1)}{16}a_{43} + \frac{(n-1)}{128}a_{52},$$

$$a_{60} = -\frac{(n-1)}{16}a_{44} + \frac{(n-1)}{72}a_{51} - \frac{(n-1)}{216}a_{56},$$

$$a_{61} = -\frac{(n-1)}{8}a_{45} + \frac{(n-1)}{32}a_{50} - \frac{(n-1)}{64}a_{55} + \frac{3(n-1)}{256}a_{57},$$

$$a_{62} = -\frac{(n-1)}{4}a_{46} + \frac{(n-1)}{8}a_{49} - \frac{(n-1)}{8}a_{54},$$

$$a_{63} = \frac{(n-1)}{4}a_{48},$$

$$a_{64} = -\frac{(n-1)}{2}a_{47},$$

$$a_{65} = -\frac{(n-1)}{4}a_{49} + \frac{(n-1)}{4}a_{54},$$

$$a_{66} = -\frac{(n-1)}{8}a_{50} - \frac{3(n-1)}{64}a_{57} + \frac{(n-1)}{16}a_{55},$$

$$a_{67} = -\frac{(n-1)}{12}a_{51} + \frac{(n-1)}{36}a_{56},$$

$$a_{68} = -\frac{(n-1)}{16}a_{52},$$

$$a_{69} = -\frac{(n-1)}{4}a_{53},$$

$$a_{70} = -\frac{(n-1)}{4}a_{54},$$

$$a_{71} = -\frac{(n-1)}{8}a_{55} + \frac{3(n-1)}{32}a_{57},$$

$$a_{72} = -\frac{(n-1)}{8}a_{57},$$

$$a_{73} = -\frac{(n-1)}{12}a_{56},$$

$$a_{74} = a_{58}r_1^{10} + a_{59}r_1^8 + a_{60}r_1^6 + a_{61}r_1^4 + a_{62}r_1^2 + \frac{a_{63}}{r_1^2} + a_{64}\ln r_1 + a_{65}r_1^2\ln r_1 + a_{66}r_1^4\ln r_1 + a_{67}r_1^6\ln r_1 + a_{68}r_1^8\ln r_1 + a_{69}(\ln r_1)^2 + a_{70}r_1^2(\ln r_1)^2 + a_{71}r_1^4(\ln r_1)^2 + a_{72}r_1^4(\ln r_1)^3 + a_{73}r_1^6(\ln r_1)^2,$$

$$a_{75} = a_{58}r_2^{10} + a_{59}r_2^8 + a_{60}r_2^6 + a_{61}r_2^4 + a_{62}r_2^2 + \frac{a_{63}}{r_2^2} + a_{64}\ln r_2 + a_{65}r_2^2\ln r_2 + a_{66}r_2^4\ln r_2 + a_{67}r_2^6\ln r_2 + a_{68}r_2^8\ln r_2 + a_{69}(\ln r_2)^2 + a_{70}r_2^2(\ln r_2)^2 + a_{71}r_2^4(\ln r_2)^2 + a_{72}r_2^4(\ln r_2)^3 + a_{73}r_2^6(\ln r_2)^2,$$

$$a_{76} = \frac{-a_{74}-a_{75}}{\ln r_1 - \ln r_2} + a_{64},$$

$$a_{77} = -a_{74} - a_{25}\ln r_1,$$

$$a_{78} = \left(\frac{r_2^4 - r_1^4}{8} + a_{25}(r_2^2\ln r_2 - r_1^2\ln r_1) - a_{25}\frac{(r_2^2 - r_1^2)}{2} + a_{27}\frac{(r_2^2 - r_1^2)}{2}\right),$$

$$
\begin{aligned}
a_{79} &= a_{29}\left(\frac{r_2^6-r_1^6}{3}\right)+a_{30}\left(\frac{r_2^4\ln r_2-r_1^4\ln r_1}{2}-\frac{(r_2^4-r_1^4)}{8}\right)\\
&\quad+a_{31}\left(\frac{r_2^4-r_1^4}{2}\right)+a_{26}\left((r_2^2\ln r_2-r_1^2\ln r_1)-\frac{(r_2^2-r_1^2)}{2}\right)+a_{28}\frac{(r_2^2-r_1^2)}{2},\\
a_{80} &= a_{58}\left(\frac{r_2^{12}-r_1^{12}}{6}\right)+a_{59}\left(\frac{r_2^{10}-r_1^{10}}{5}\right)+a_{60}\left(\frac{r_2^8-r_1^8}{4}\right)+a_{61}\left(\frac{r_2^6-r_1^6}{3}\right)\\
&\quad+a_{62}\left(\frac{r_2^4-r_1^4}{2}\right)-2a_{63}\left(\frac{1}{r_2}-\frac{1}{r_1}\right)+a_{65}\left(\frac{r_2^4\ln r_2-r_1^4\ln r_1}{2}-\frac{(r_2^4-r_1^4)}{8}\right)\\
&\quad+a_{66}\left(\frac{r_2^6\ln r_2-r_1^6\ln r_1}{3}-\frac{(r_2^6-r_1^6)}{18}\right)+a_{67}\left(\frac{r_2^8\ln r_2-r_1^8\ln r_1}{4}-\frac{(r_2^8-r_1^8)}{32}\right)\\
&\quad+a_{68}\left(\frac{r_2^{10}\ln r_2-r_1^{10}\ln r_1}{5}-\frac{(r_2^{10}-r_1^{10})}{50}\right)\\
&\quad+a_{69}\left(r_2^2(\ln r_2)^2-r_1^2(\ln r_1)^2-r_2^2(\ln r_2)-r_1^2(\ln r_1)+\frac{(r_2^2-r_1^2)}{2}\right)\\
&\quad+a_{70}\left(\frac{r_2^4(\ln r_2)^2-r_1^4(\ln r_1)^2}{2}\frac{-r_2^4(\ln r_2)+r_1^4(\ln r_1)}{4}+\frac{(r_2^4-r_1^4)}{16}\right)\\
&\quad+a_{71}\left(\frac{r_2^6(\ln r_2)^2-r_1^6(\ln r_1)^2}{3}\frac{-r_2^6(\ln r_2)+r_1^6(\ln r_1)}{9}+\frac{(r_2^6-r_1^6)}{54}\right)\\
&\quad+a_{72}\left(\frac{r_2^6(\ln r_2)^3-r_1^6(\ln r_1)^3}{3}\frac{-r_2^6(\ln r_2)^2+r_1^6(\ln r_1)^2}{6}+\frac{r_2^6(\ln r_2)-r_1^6(\ln r_1)}{18}-\frac{(r_2^6-r_1^6)}{108}\right)\\
&\quad+a_{73}\left(\frac{r_2^8(\ln r_2)^2-r_1^8(\ln r_1)^2}{4}+\frac{r_2^8(\ln r_2)+r_1^8(\ln r_1)}{16}-\frac{(r_2^8-r_1^8)}{128}\right)\\
&\quad+a_{76}\left(r_2^2\ln r_2-r^2\ln r_1-\frac{(r_2^4-r_1^4)}{2}\right)+a_{77}(r_2^2-r_1^2).
\end{aligned}
$$

[1] T. W. Latham, Fluid motion in a peristaltic pump, M. Sc. Thesis, Massachusetts Institute of Technology, Cambridge 1966.

[2] A. El. Hakeem, A. E. I Naby, A. E. M. El Misery, and I. I. El Shamy, Physica A **343**, 1 (2004).

[3] S. Nadeem and N. S. Akbar, Commun. Nonlinear Sci. Numer. Simul. **14**, 3844 (2009).

[4] S. Srinivas and M. Kothandapani, Int. Commun. Heat Mass Transf. **35**, 514 (2008).

[5] S. Nadeem, T. Hayat, N. S. Akbar, and M. Y. Malik, Int. Commun. Heat Mass Transf. **52**, 4722 (2009).

[6] S. Nadeem and N. S. Akbar, Commun. Nonlinear Sci. Numer. Simul. **14**, 4100 (2009).

[7] S. Srinivas and R. Gayathri, Appl. Math. Comput. **215**, 185 (2009).

[8] S. Srinivas and M. Kothandapani, Appl. Math. Comput. **213**, 197 (2009).

[9] S. Srinivas, R. Gayathri, and M. Kothandapani, Comput. Phys. Commun. **180**, 2115 (2009).

[10] A. El. Hakeem, A. E. I. Naby, A. E. M. El Misery, and I. I. El Shamy, Appl. Math. Comput. **128**, 19 (2002).

[11] M. Ealshahed and M. H. Haroun, Math. Probl. Eng. **6**, 663 (2005).

[12] T. Hayat, N. Ali, and S. Asghar, Appl. Math. Comput. **188**, 1491 (2007).

[13] Y. Wang, T. Hayat, N. Ali, and M. Oberlack, Physica A **120**, 1291 (2007).

[14] M. Kothandapani and S. Srinivas, Int. J. Nonlinear Mech. **43**, 915 (2008).

[15] A. El. Hakeem, A. E. I. Naby, A. E. M El. Misery, and I. I. El Shamy, J. Phys. A **36**, 8535 (2003).

[16] S. Nadeem and S. Akram, Commun. Nonlinear Sci. Numer. Simul. **15**, 1705 (2010).

[17] N. T. M. Eldabe, M. F. El-Sayed, A. Y. Ghaly, and H. M. Sayed, Archive Appl. Mech. **78**, 599 (2007).